# The Influence of Channel Aspect Ratio on Performance of Optimized Thermal-Fluid Structures

Ercan M. Dede[1*]
[1]Technical Research Department, Toyota Research Institute of North America
*Corresponding author: Toyota Motor Engineering & Manufacturing of North America, Inc., 1555 Woodridge Ave., Ann Arbor, MI, 48105. Email address: eric.dede@tema.toyota.com

**Abstract:** This paper presents a parametric geometry study of a thermal-fluid structure for single phase liquid cooling applications. Topology optimization results for an example two-dimensional system are first presented. The results of numerical experiments examining the influence of channel aspect ratio, i.e. height over width, on the thermal-fluid performance of a derived branching channel cold plate are then explained. These results are compared with those for a similarly sized straight microchannel cold plate. The optimized structure is found to exhibit moderately higher thermal resistance in addition to significantly lower pressure drop when compared with the traditional straight channel system. The study highlights an analysis and design method that combines optimization techniques with further design refinement via automated geometry parameter sweeps.

**Keywords:** Microchannel, heat transfer, liquid cooling

## 1. Introduction

Single phase liquid cooled microchannel heat sink technologies have received significant attention due to their potential for handling very high heat fluxes [1,2]. Comprehensive research has shown that traditional straight channel systems may exhibit very low thermal resistance at the cost of relatively high pressure drop [3]. Alternatively, novel heat sink designs have been proposed to reduce the pressure drop penalty while maintaining some of the heat transfer benefits of straight microchannels [4,5]. Accordingly, this paper examines the effects of channel aspect ratio on the performance of a non-straight branching channel cold plate design developed from thermal-fluid topology optimization results.

The paper is organized as follows. In Section 2 the governing equations for heat transfer and fluid flow are provided along with a review of the topology optimization model and results. Two geometric parameter studies are then described in Section 3. The first study examines the channel aspect ratio of the branching channel cold plate while the second study is focused on a similarly sized straight channel system. The results of both studies are then reported in Section 4. Discussion and conclusions are provided in Sections 5 and 6, respectively.

## 2. Governing Equations

Conjugate heat transfer is assumed in all of the following parameter studies. Thus, the governing equations in vector form, per [6], for single phase convective heat transfer and flow in the fluid domain are

$$\nabla \cdot (k \nabla T) + Q = \rho C (\mathbf{u} \cdot \nabla T), \tag{1}$$

$$\nabla \cdot \mathbf{u} = 0, \tag{2}$$

$$\rho (\mathbf{u} \cdot \nabla \mathbf{u}) = -\nabla P + \nabla \cdot \left\{ \mu \left[ (\nabla \mathbf{u}) + (\nabla \mathbf{u})^{\mathbf{T}} \right] \right\}, \tag{3}$$

where $\mathbf{u}$ is the fluid velocity vector, $T$ is the temperature state variable, and $P$ is the fluid pressure variable. The thermal conductivity, density, specific heat capacity, and dynamic viscosity of the fluid are given by $k$, $\rho$, $C$, and $\mu$, respectively.

In the case of the solid region $\mathbf{u} = 0$ (i.e. zero fluid velocity) and Eqn. (1) reduces to

$$\nabla \cdot (k_s \nabla T) + Q_s = 0, \tag{4}$$

where the subscript, s, denotes the solid domain.

### 2.1 Optimization Model

The model described in this section builds on prior work related to the topology optimization of thermal-fluid systems using a COMSOL-MATLAB (v.3.5a) script, [7]. The reader is referred to the literature for greater details on this and similar optimization methods [8-13].

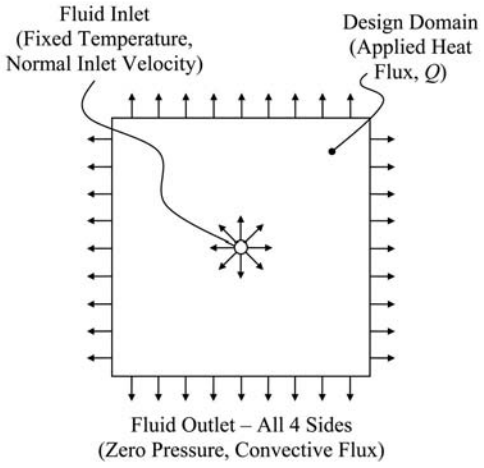


**Figure 1:** 2-D model of a thin heated plate with boundary conditions and loads.

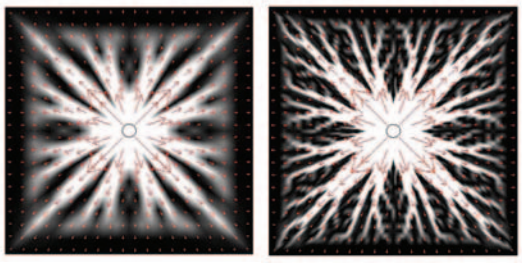

**Figure 2:** Optimal cooling channel layouts for coarse (left) and fine (right) meshes using 40% fluid volume fraction (arrows denote fluid velocity vectors).

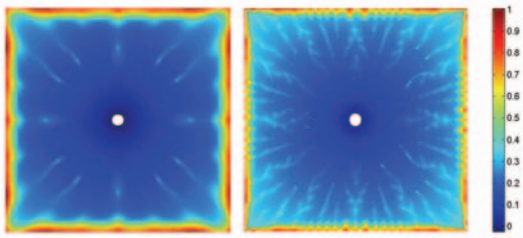

**Figure 3:** Normalized temperature contours for coarse (left) and fine (right) meshes.

For this work, the optimization method described in [7] was applied, and the mean temperature and fluid power dissipated in the design domain were minimized. A square two-dimensional (2-D) design domain representing a very thin heated plate was assumed. This 2-D model was used since a typical microchannel cooling system has in-plane dimensions that greatly exceed its out-of-plane thickness.

The implemented model is shown in Fig. 1 along with applied boundary conditions and loads. A laminar flow (i.e. Re < 2000), fixed temperature inlet velocity condition was specified along with a zero pressure, convective flux outlet condition. A uniform heat flux was applied to the design domain.

The optimal topology for this model was computed using both fine and coarse meshes having 2,880 and 25,000 degrees of freedom, respectively, to examine the effect of mesh refinement on the final topology. The corresponding optimization results are presented in the next section.

### 2.2 Optimization Results

The optimal channel topologies for the model described in Section 2.1 are shown in Fig. 2, where the coarse mesh result is on the left and the fine mesh result is on the right [14]. A 40% fluid volume fraction was used in both cases. Observe that a branching channel structure is obtained, and finer mesh refinement produces a higher level of branching complexity.

Figure 3 shows the normalized temperature contour results for both mesh conditions. Note that the ratio of the weightings for the thermal to fluid portions of the objective function is approximately 30:1, (see [7] for further details). These results illustrate the manner in which the branching channel structure decreases the temperature of the design domain through effective fluid delivery. Consequently, the insulative porous solid material is forced out towards the edges of the domain regardless of the magnitude of the inverse permeability. The main diagonal branches of both structures then work to reduce the maximum temperature which tends to occur in the isolated corners of the domain.

The coarse mesh topology optimization result from Fig. 2 (left hand side) is used in the development of a cold plate structure and the subsequent geometric parameter studies.

## 3. Geometric Parameter Study

Figure 4 shows a one-quarter symmetry solid model of the geometry for the branching channel cold plate. The model geometry consists of a jet

plate (shown transparent) with a center nozzle that directs the coolant downwards into the channel structure, through the radial branching channels, and then out through the sides of the cold plate. Note that the channel geometry in this figure was derived from the coarse mesh result provided in Fig. 2 (left hand side).

The coarse mesh result was employed due to the relatively small overall size of the cold plate. Specifically, the size of the full plate is 17.2 mm square with a 1.26 mm initial thickness. The initial channel height, *h*, was set to 0.5 mm and was swept from this initial value up to 2.0 mm in 0.5 mm increments using the COMSOL 4.0a 'parametric sweep' feature. The cold plate channel width, *w*, ranges from approximately 0.66 to 2.42 mm. By using the coarse mesh result to develop the cold plate, the overall complexity of the microscale channel system is reduced.

For comparison purposes, a straight microchannel cold plate was also studied. A symmetry model of a single microchannel representing a 17.2 mm square cold plate with an initial thickness 1.26 mm is shown in Fig. 5. The channel width was set equal to the minimum channel width of the branching cold plate design, i.e. 0.66 mm, while the channel height was again swept from 0.5 to 2 mm in 0.5 mm increments.

In both cases, the channel aspect ratio was assumed as the channel height divided by the minimum channel width, $\gamma = h / w_{min}$. Therefore, four separate values of the channel aspect ratio (~0.75, 1.5, 2.25, and 3) were considered for each of the described computational models.

### 3.1 Computational Model Description

Each of the models shown in Figs. 4 and 5 were imported into COMSOL 4.0a using the CAD geometry LiveLink feature. For each finned cold plate channel structure a thermally conductive material was assumed having a thermal conductivity, specific heat capacity, and density of 160 W/(m·K), 900 J/(kg·K), and 2700 kg/m$^3$, respectively. The coolant fluid thermal conductivity, specific heat capacity, density, and dynamic viscosity at 65ºC were, respectively, set to 0.654 W/(m·K), 4182 J/(kg·K), 982 kg/m$^3$, and 4.4E-4 Pa·s. An insulative material was also assumed for the jet plate and straight microchannel cap with a thermal conductivity of 0.26 W/(m·K), a specific heat capacity of 1700 J/(kg·K), and a density of 1150 kg/m$^3$.

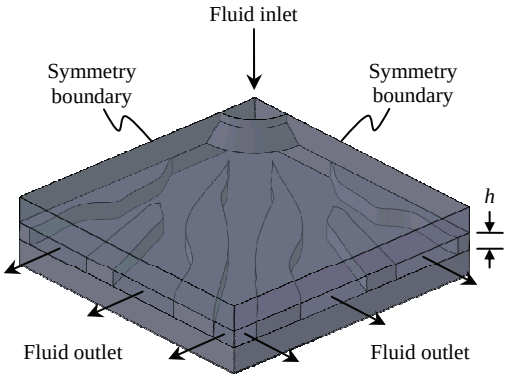


**Figure 4:** One-quarter symmetry solid model for branching channel cold plate (arrows indicate fluid flow direction; *h* represents the channel height).

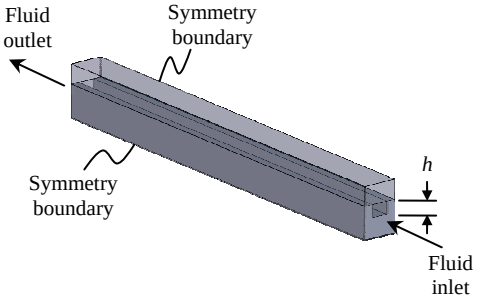


**Figure 5: S**ymmetry solid model for a straight microchannel cold plate (arrows indicate fluid flow direction; *h* represents the channel height).

Appropriate symmetry boundary conditions were applied to each of the models described in Figs. 4 and 5. Additionally, a uniform heat flux, $q$ = 100 W/cm$^2$, was applied to the bottom side of each channel structure. The fluid inlet temperature was fixed to 65 ºC. A zero pressure, convective flux condition was set at each fluid outlet boundary.

An automated parameter study was set up to sweep the height parameter, *h*, in each model from 0.5 to 2 mm, as described in the prior section. The computational models were solved at each channel height parameter step over a range of fluid inlet volumetric flow rates spanning 0.025 to 0.15 L/min.

## 4. Parameter Study Results

The temperature contour results for the branching cold plate with a 0.5 mm channel height at maximum inlet fluid flow rate are shown in Fig. 6. Likewise, the results for the straight channel structure are shown in Fig. 7. Observe that the maximum temperature for the branching channel design, 110 ºC, occurs at the outside corners of the square plate. For the straight channel design the maximum temperature, 119 ºC, occurs at the end of the channel after the thermal boundary layer is fully developed.

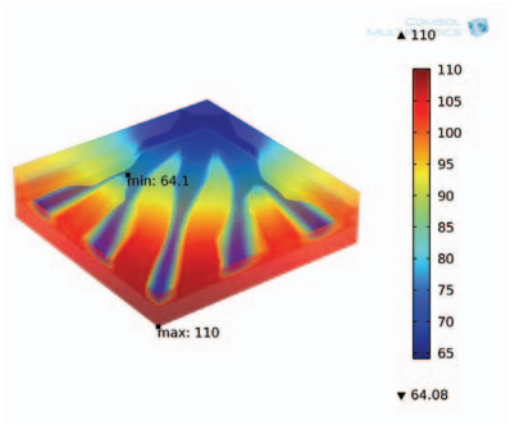


**Figure 6:** Temperature contour results for branching microchannel cold plate with 0.15 L/min flow rate and 0.5 mm channel height (shown transparent for clarity).

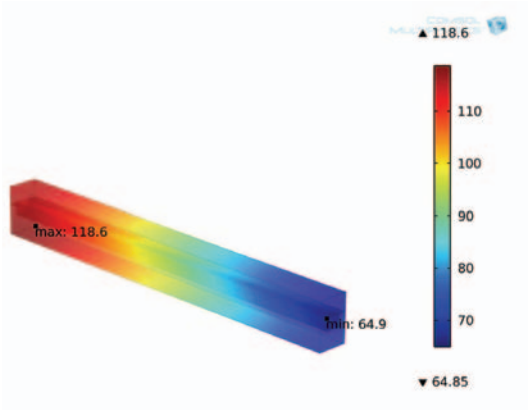


**Figure 7:** Temperature contours for straight microchannel cold plate with 0.15 L/min flow rate and 0.5 mm channel height (shown transparent for clarity).

Two performance metrics are used to evaluate the effectiveness of each of the cold plate designs over the various height parameters and flow rate ranges. First, the thermal resistance, $R_{th}$, of each cold plate is calculated using Eqn. (5).

$$R_{th} = \frac{T_{\max} - T_f}{q} \tag{5}$$

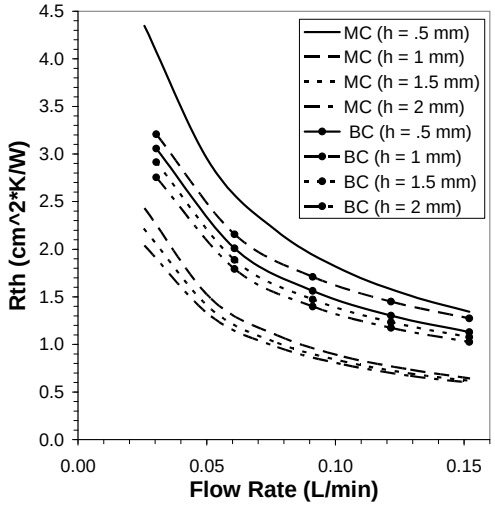


**Figure 8:** Comparison of thermal resistance for branching (BC) and straight microchannel (MC) cold plates.

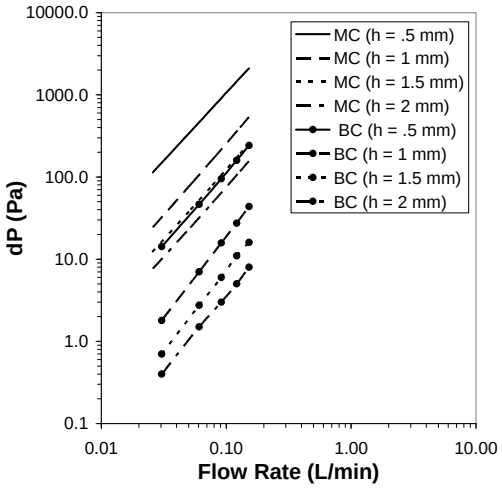


**Figure 9:** Comparison of pressure drop for branching (BC) and straight microchannel (MC) cold plates.

In Eqn. (5) $T_{max}$ is the maximum cold plate temperature, $T_f$ is the fluid inlet temperature, and $q$ is the applied heat flux. The second performance metric is the maximum pressure drop which is calculated as the difference between the computed inlet pressure and the fixed outlet pressure; $\Delta P = P_{in} - P_{out}$.

Figure 8 provides the thermal resistance as a function of flow rate for both cold plates over all channel height parameter values. The thermal resistance of the branching microchannel cold plate for $h$ = 0.5 mm is less than that for the straight microchannel system. However, as the height and channel aspect ratio is increased the thermal resistance of the straight microchannel system drops to values that are approximately one-half of those for the branching microchannel system. Additionally, the branching channel cold plate thermal resistance increases as channel height is increased from 0.5 to 1 mm. However, as the channel height is further increased to 1.5 and 2 mm the thermal resistance then progressively decreases.

The pressure drop as a function of flow rate for both cold plate designs is shown in Fig. 9. Observe that at the 0.5 mm channel height the branching cold plate design exhibits a maximum pressure drop value of 0.24 kPa compared with 2.1 kPa for the straight microchannel design. This trend in magnitude is consistent across the various channel aspect ratios where the branching microchannel cold plate generally exhibits one to two orders of magnitude lower pressure drop.

## 5. Discussion

While the straight microchannel system outperforms the branching channel structure in terms of heat transfer at larger channel aspect ratios, the considerably larger $\Delta P$ may be prohibitive in applications where pumping power is limited. This characteristic of microchannels is well known, and it is a primary obstacle to widespread application [3].

Thus, the results presented in this paper demonstrate an integrated optimization, analysis and design procedure resulting in a branching channel cold plate design that provides moderate heat transfer with almost negligible pressure drop. Even so, careful consideration should be given to the tradeoffs between heat sink geometric (i.e. manufacturing) complexity, cost of implementation, and the desired thermal-fluid performance.

## 6. Conclusions

In this paper a set of thermal-fluid topology optimization results for a thin heated plate with a center fluid inlet was reviewed. These results were utilized in the development of a branching microchannel cold plate design. The heat transfer performance of this cold plate was examined and compared with the performance of a traditional straight microchannel system across designs having different channel aspect ratios. Generally, the results indicate that the branching channel structure provides moderately lower heat transfer enhancement with nearly negligible pressure drop in comparison to the straight microchannel system.

This numerical study illustrates an analysis and design method that combines optimization techniques with further design refinement via automated geometry parameter sweeps. The method is broad and may be applied to the design of various vehicle electromechanical systems.

## 7. References


1. D.B. Tuckerman and R.F.W. Pease, High-performance heat sinking for VLSI, *IEEE Electronic Devices Letters*, EDL-2, pp. 126-129 (1981).
2. C.B. Sobhan and S.V. Garimella, A comparative analysis of studies on heat transfer and fluid flow in microchannels, *Microscale Thermophysical Engineering*, 5, pp. 293-311 (2001).
3. S.V. Garimella and V. Singhal, Single-phase flow and heat transport and pumping considerations in microchannel heat sinks, *Heat Transfer Engineering*, 25, pp. 15-25 (2004).
4. G.M. Harpole and J.E. Eninger, Micro-channel heat exchanger optimization, In Proceeding of the *7th IEEE SEMI-THERM Symposium*, pp. 59-63 (1991).
5. F.P. Incropera, *Liquid Cooling of Electronic Devices by Single-Phase Convection*, John Wiley & Sons, New York, pp. 217-252 (1999).
6. J.N. Reddy and D.K. Gartling, *The Finite Element Method in Heat Transfer and Fluid Dynamics*, CRC Press, Boca Raton, pp. 7-10 (2000).

7. E.M. Dede, Multiphysics topology optimization of heat transfer and fluid flow systems, In proceedings of the *COMSOL Users Conference*, (2009).
8. T. Borvall and J. Petersson, Topology optimization of fluids in Stokes flow, *International Journal for Numerical Methods in Fluids*, 41, pp. 77–107 (2003).
9. M.P. Bendsoe and O. Sigmund, *Topology Optimization - Theory, Methods and Applications*, Springer Verlag, Berlin, pp. 111–113 (2003).
10. L.H. Olesen, F. Okkels, and H. Bruus, A high-level programming-language implementation of topology optimization applied to steady-state Navier-Stokes flow, *International Journal for Numerical Methods in Engineering*, 65, pp. 975–1001 (2006).
11. C.S. Andreasen, A.R. Gersborg, and O. Sigmund, Topology optimization for microfluidic mixers, *International Journal for Numerical Methods in Fluids*, 61, pp. 498–513 (2008).
12. A.S. Iga, S. Nishiwaki, K. Izui, and M. Yoshimura, Topology optimization for thermal conductors considering design-dependent effects, including heat conduction and convection, *International Journal of Heat and Mass Transfer*, 52, pp. 2721-2732 (2009).
13. G.H. Yoon, Topological design of heat dissipating structure with forced convective heat transfer. *Journal of Mechanical Science and Technology*, 24, pp. 1225–1233 (2010).
14. E.M. Dede, Multiphysics optimization of hierarchical thermal-fluid structures, In Proceedings of the 9th World Congress on Computational Mechanics and 4th Asian Pacific Congress on Computational Mechanics, p. 292 (2010).